Catena 218 (2022) 106540

Contents lists available at ScienceDirect

Catena

journal homepage: www.elsevier.com/locate/catena

Testing of a commercial vector network analyzer as low-cost TDR device to measure soil moisture and electrical conductivity

David Moret-Fernández [a,*], Francisco Lera [b], Borja Latorre [a], Jaume Tormo [c], Jesús Revilla [d]

[a] Estación Experimental de Aula Dei, Consejo Superior de Investigaciones Científicas (EEAD-CSIC), POB 13034, 50080 Zaragoza, Spain
[b] Instituto de Investigación en Ingeniería de Aragón, University of Zaragoza, 50018 Zaragoza, Spain
[c] Technical School and Environmental Sciences Institute, University of Zaragoza, 22071 Huesca, Spain
[d] Instituto Pirenaico de Ecología (CSIC), Avda. Nuestra Señora de la Victoria, 16, Jaca, Spain

ARTICLE INFO

Keywords:
Vector network analyzer
Time domain reflectometry
Apparent permittivity
Soil water content
Soil electrical conductivity

ABSTRACT

Time Domain Reflectometry (TDR) is a non-destructive technique to determine the soil apparent dielectric constant, ε_a, the volumetric water content, θ, and bulk electrical conductivity, σ. However, the high cost of TDR devices may limit its use. This study evaluates two different low-cost Vector Network Analyzers (VNA) commercially available (NanoVNA), with 1.5 (VNA1.5) and 3.0 (VNA3.0) GHz maximum operating frequency. NanoVNA can be used for measurements of Frequency Domain Reflectometry (FDR) or, after suitable post-processing, for θ and σ TDR measures. Although FDR and TDR are dual procedures, TDR is easier to interpret for soil experiments. The TDR waveforms and ε_a measured with NanoVNA connected to 10 and 20 cm length three-rod probes immersed in air, distilled water, and a soil column with different θ were compared to those measured using a TDR100 (Campbell Sci.) instrument. The capacity of VNAs to measure σ was evaluated by immersing a 10 cm length three-rod probe in different NaCl-water solutions. Measurements obtained with the VNA and TDR100 were compared in a field test using two-rod 22 cm length TDR probes inserted in soil plots with increasing water content. A robust fit was observed between TDR waveforms registered with the two VNAs and the TDR100. Although VNA3.0 doubles the frequency range of VNA1.5, both devices allowed for good estimates of ε_a ($\varepsilon_{aVNA1.5,\ 3.0} = 1.001\ \varepsilon_{aTDR100} - 0.2125$; $R^2 = 0.999$). These results indicate that the low-cost VNA devices can measure soil water content with similar accuracy and precision as the TDR100. A good agreement ($\sigma_{VNA1.5,\ 3.0} = 0.999\ \sigma_{CM} + 0.0023$; $R^2 = 0.999$) was also observed between the σ measured using a conductivity meter (CM) and that estimated with the VNAs. Finally, a good correlation was also observed between θ measured in the field experiment with TDR100 and the VNA1.5 and VNA3.0 devices.

1. Introduction

Time domain reflectometry (TDR) and frequency domain reflectometry (FDR) techniques, based on the measurement of apparent permittivity (ε_a), have been widely used for real-time and in situ estimation of volumetric water content. of the soil (θ) and the global electrical conductivity (σ). For this, TDR and FDR hardware designed and marketed mainly for the telecommunications industry, together with suitable probes for ground measurements, have been commonly used.

The hardware used for FDR is the Vector Network Analyzer (VNA). This instrument is commonly used in high frequency technology laboratories worldwide to characterize radiofrequency components, devices, circuits, and sub-assemblies. A review of VNA history, operation, applications and limitations can be found in chapter 5 of Sayed and Martens (2013). The first commercial VNAs reached the market in the 1960's and have evolved since then to the highly sophisticated equipment needed by the telecommunications technology industry nowadays. Most of today VNAs are two-port devices. The reflection port, which functions as output and input, is connected with a transmission line to the input of the Device Under Test (DUT). This port generates an incident signal, usually a linear or logarithmic frequency swept electromagnetic wave. Simultaneously, the reflecting port, working as input to the VNA, measures the phase and amplitude of the signal reflected in the DUT. The transmission port, when used, works as an extra input also connected with a transmission line to the output of the DUT. The transmission port measures the phase and amplitude of the signal that

* Corresponding author.
E-mail address: david@eead.csic.es (D. Moret-Fernández).

https://doi.org/10.1016/j.catena.2022.106540
Received 17 May 2022; Received in revised form 20 July 2022; Accepted 22 July 2022
Available online 1 August 2022

passes through the DUT. The VNA computes, stores and displays the scattering parameters of the DUT: S_{11} (the reflection coefficient) and S_{21} (the transmission coefficient). S_{11} and S_{21} are defined as the dimensionless complex ratio of the reflected or transmitted signal to the incident signal, respectively, measured for each frequency step. This process can be repeated several times to improve the signal to noise ratio by averaging if desired.

The measurement of S_{11} with a VNA determines the frequency dependent complex input impedance $Z_{in}(\omega)$ of a circuit (for instance a cable length ending in a probe inserted into the soil) connected to its reflection port. The result is referred to the system characteristic impedance R_0 (50 Ω in most cases):

$$S_{11}(\omega) = \frac{Z_{in}(\omega) - R_0}{Z_{in}(\omega) + R_0}$$

On the other side, a TDR generates a fast-rising step excitation that travels along the cable-probe circuit, recording at a high sampling rate the reflected signal for a time long enough to account for the possible multiple reflections. The output is presented as a time-dependent reflection coefficient $S_{11}(t)$ also referred to the system characteristic impedance R_0. We will use the equivalent denominations $\rho(\omega) \equiv S_{11}(\omega)$ and $\rho(t) \equiv S_{11}(t)$ for the reflection coefficients in the rest of the text, since they are in common use in the field of soil science.

The VNA-measured complex $\rho(\omega)$ can be transformed to an equivalent $\rho(t)$ as being measured with a virtual TDR. Vice-versa, $\rho(t)$ data obtained with TDR hardware can be translated to the frequency domain for further analysis. The main advantage of the analysis in the frequency domain is the possibility of using realistic transmission line models of the cable-probe assembly. In (Heimovaara 1994) and (Friel and Or 1999) the analysis of TDR data is made in the frequency domain to be able to extract the frequency-dependent complex permittivity of soils. Huisman et al (2002) satisfactorily compared a direct analysis of travel time measurements in TDR data with synthetic TDR waveforms obtained from frequency domain calculations in soil models with frequency dependent permittivity. Later, Huisman et al. (2004) also compared TDR and direct VNA measurements of soil complex permittivity made in the frequency domain. In this work, we will apply the opposite approximation: the transformation of VNA frequency domain measurements to the time domain. Although $\rho(\omega)$ can can be directly used to estimate θ and σ in soils, the analysis required to separate probe from cable effects is noticeably more complex in FDR than in TDR. Moreover, this transformation allows the use of VNA devices as a direct replacement of TDR instruments for soil characterization experiments under specific working conditions.

A great advantage of TDR is its ability to make non-destructive, rapid and continuous measurements of both σ and θ with a single probe and in the same sampling volume (He et al., 2021). Determination of θ is based on the time required by the electrical signal to travel and reflect back along the probe's rods (Topp et al., 1980). In contrast, σ is estimated from the long-time TDR waveform analysis (Lin et al., 2008). Another advantage of the TDR technique is the simplicity of the probes, which allows to design and manufacture its own probes. For instance, a TDR probe may consist on a two or three simple stain-steel wires inserted into the soil (Miyamoto et al. 2001). This makes the probes inexpensive and well suited for large-scale water content measurements. This great versatility to manufacture TDR probes allows, for example, to make discontinuous probes for soil water profiles (Topp et al., 1982), non-invasive sensors to estimate soil surface water content (Selker et al., 1993) or soil sensors to measure the matrix water potential (Or and Wraith, 1999) or the electrical conductivity of the soil water solution (Moret-Fernández et al., 2012). Furthermore, modeling of the TDR signal also allows estimation of the soil water profile from the inverse analysis of a single waveform recorded with a long probe inserted vertically into the soil (Greco 2006).

Since its first application for soil water profiling in the 1980s, the TDR technology has evolved towards more accurate and portable instruments. For example, the 1502C Metallic Cable Tester, manufactured by Tektronix of Beaverton, Oregon, was the first device used for soil field research. This instrument incorporated a small LCD screen to identify the inflection points of the TDR waveform. Because the manual waveform analysis performed with the 1502C Tektronix was inaccurate and time-consuming, additional software for TDR analysis was developed, e.g., TACQ (Evett, 2000), WinTDR (Jones et al., 2002) or the TDR-LAB (Moret-Fernández et al., 2010). Although these programs allow accurate determination of the soil water content, the weight and volume of the TDR instruments plus a laptop running the software could limit its use in field measurements. To date, many companies make and commercialize TDR instruments for soil applications: Adcon, Vienna, Austria, Streat Drycom, Bradford, UK, Campbell Scientific Inc., Logan, UT, USA, Stetel srl, LI, Italy, Meteolabor, Wetzikon, Switzerland, Soilmoisture Equipment Corp., California. USA, among others. Recently, Villoro et al. (2021) presented TDR-WiFi, a small system that can be used with TDR100 (Campbell Scientific) devices and allows a convenient use under field conditions because their reduced volume and weight.

Although these recent developments make the TDR technique more portable and facilitate the use of these devices in difficult to access areas, the high cost of TDR instruments (around 4000 €, depending on the model) may still limit their use in some scenarios. To overcome this potential limitation, a recent work of Qiwei et al. (2019) proposed using a mini vector network analyzer (miniVNA) for soil moisture measurement. MiniVNA is a quantum leap in electromagnetic technology, with a relatively small size and a fraction of the cost of standard tabletop VNAs (between 50 and 100 € unit^{-1}). In this case, the miniVNA, which operated between 1 MHz and 3 GHz, was connected to a standard 0.60-cm thickness telescopic very high frequency (VHF) radio communication monopole antenna. Although this new technology showed a response to the soil water content, the relatively low R^2 value obtained in the calibration model could be explained by the fact that the antenna probe was not specifically designed for measuring soil moisture but for radio communication. Using an open-ended coaxial probe, González-Teruel et al. (2022) evaluated the NanoVNA for dielectric measurements within the frequency domain. Results showed that the accuracy of the NanoVNA was comparable to that of a commercial VNA between 1 and 500 MHz according to tests in reference organic liquids, while a lack of stability was found beyond 700 MHz. The dielectric response of the soils approximated the well-known Topp et al. (1980) equation at high frequencies. However, in those latter studies, no evaluation of the NanoVNA for soil bulk electrical conductivity measures was performed.

Given the promising capabilities of NanoVNAs for soil water content measures, this study evaluates two different small volume and low-cost NanoVNA, NanoVNA of 1.5 (VNA1.5) and 3.0 (VNA3.0) GHz, for measuring soil θ and σ. However, unlike to the previous NanoVNA studies, which worked in the Frequency Domain, the soil water content and bulk electrical conductivity are here analyzed within the Time Domain, using two- and three-rod probes. The results (i.e., derived TDR waveforms and measured θ) obtained with these VNA devices connected to a 10 and 20 cm length three-rod probes immersed in air, distilled water, and a soil column with different values of θ were compared to those measured with a TDR100 (Campbell Sci.) cable tester. Analogously, the accuracy of NanoVNAs to measure σ was evaluated by immersing a 10 cm length three-rod probe in different NaCl-water solutions. Finally, the NanoVNA devices were tested and compared to the TDR100 in a water content measurement field trial.

2. TDR analysis of FDR measurements

The analysis of TDR and FDR measurements in soils is usually carried out under the assumption that the cable-probe assembly behaves as a Linear Time Invariant (LTI) causal system. This assumption is indeed valid for the weak electromagnetic fields involved in these measurements. From general LTI systems theory (Oppenheim et al., 1997), a LTI

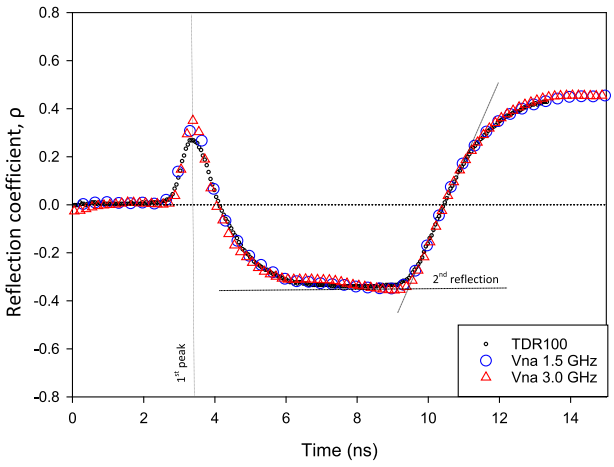

Fig. 1. TDR waveforms recorded with TDR100 and VNA1.5 and 3.0 devices connected to a 10 cm length TDR probe immersed in distilled water.

system is fully characterized by its unit impulse response *h(t)*. The response of the system to any excitation *x(t)* can be obtained applying the convolution theorem:

$$y(t) = x(t)^{*}h(t) = \int_{-\infty}^{t} x(\tau)h(t-\tau)d\tau$$

The * symbol stands for convolution. For LTI systems, convolution is a commutative operation and then $x(t)^{*}h(t) = h(t)^{*}x(t)$.

In TDR measurements, the excitation signal is not an impulse but a step. The unit-step is defined as $u(t) = 1$ for $t > 0$ and $u(t) = 0$ for $t < 0$. In systems theory, the unit impulse is represented with a Dirac delta generalized function, and thus the unit step $u(t)$ and the unit impulse are related as:

$$u(t) = \int_{-\infty}^{t} \delta(\tau)d\tau$$

This expression can be interpreted in the LTI context as follows: the unit step function $u(t)$ is the impulse response of an integrator. The step response $s(t)$ of a LTI system with impulse response $h(t)$ is $s(t) = u(t)^{*}h(t)$. Applying the commutative property of convolution, $s(t) = h(t)^{*}u(t)$, which equals the response of an integrator (with impulse response $u(t)$) to the input $h(t)$. That is, the unit step response of a LTI system is the running integral of its impulse response:

$$s(t) = \int_{-\infty}^{t} h(\tau)d\tau$$

When making TDR or FDR measurements, the reflection coefficient are recorded as a discrete series of data. In the time domain, N TDR data points are registered at a selectable high sampling rate (F_s) and thus consecutive data points are separated by a short time interval ($\Delta t = 1/F_s$). The maximum sampling rate available is device-dependent and is limited by the rise time of the exciting step, the slew rate of the input amplifiers and the A/D subset working rate. Higher sampling rates provide finer temporal resolution and consequently shorter probes can be used. For the conductivity estimation at longer times after the excitation, the sampling rate can be decreased. Notice however, that decreasing the sampling rate does not reduce the high frequency content of the exciting step. In a VNA, when the aim is to transform the measured reflection coefficients to an equivalent virtual TDR instrument output, N FDR data points are recorded in a linear frequency sweep from F_{min} (the lowest operating frequency available of the VNA) to F_{max}, and thus consecutive data points are separated by a frequency interval $\Delta F = (F_{\max} - F_{\min})/N \approx F_{\max}/N$. The maximum and minimum operating frequencies are device-dependent. In this work the possible values for $F_{\max}$ are 1,5 or 3 GHz and for $F_{\min}$ 10 or 50 KHz, depending on the hardware used, and thus the above approximation for ΔF is good to parts in 10^5.

As already mentioned, for causal LTI systems, the time domain response to a step excitation is the time integral of the impulse excitation response. Thus, to compute the TDR response from the FDR data, a synthetic ideal impulse excitation is Fourier transformed to the frequency domain, which is then multiplied by the complex FDR data that represents the frequency response of the circuit and the result is numerically integrated. The real part of the resulting data series constitutes the virtual TDR response.

As both TDR and FDR signals are discrete, the Discrete Fourier Transform (DFT) and the Inverse Discrete Fourier Transform (IDFT) should be used to swap from the time domain to the frequency domain and vice-versa. The theory of DFT and IDFT can be found in signal processing textbooks (i.e. Oppenheim et al., 1997), and its application to TDR measurements is explained in several of the cited works (Heimovaara 1993; Heimovaara 1994; Friel and Or 1999; Huisman et al., 2002). In practice, both transformations are computed by well-known highly efficient algorithms (Cooley and Tukey, 1965) nowadays named Fast Fourier Transform (FFT) and Inverse Fast Fourier Transform (IFFT). Implementations of these algorithms are included in many mathematical packages, libraries and in Digital Signal Processing (DSP) chipsets. The detailed implementation used in this study to obtain the TDR waveforms from the FDR dataset can be found in Section 3.1.

Starting with a N points FDR array sweep from F_{min} to a maximum frequency $F_{max} \gg F_{min}$, the process ends up with a M = 2 N-1 TDR array with a time resolution of $1/(2F_{max})$, that is, approximately 333 ps for VNA1.5 and 167 ps for VNA3.0 measured datasets. Notice that increasing the frequency resolution of the FDR sweep results only in a longer TDR array but not in a finer time resolution. The resulting VNA time resolution is coarser than the 12 ps best resolution of the Campbell TDR100 but, as we will show in the following sections, it is enough for soil characterization using probes of 10 cm length or longer.

Determination of θ from TDR waveform is based on previous calculus of ε_a, estimated according to (Topp et al., 1980).

$$\varepsilon_a = \left(\frac{ct_L}{2L}\right)^2 \quad (1)$$

where c (3×10^8 m/s) is the light speed, L (m) is the length of the probe rod embedded in some media, and t_L (s) is the two-way pulse travel time along L. The travel time is the difference between the time at which the signal enters the TDR probe's rods (first peak) and the time when it arrives at the end of the TDR probe's rods (second reflection point) (Fig. 1). Among the different methods to determine this last point (He et al., 2021), the tangent procedure (Heimovaara, 1993) was employed. Then, the Topp et al. (1980) polynomial function is generally employed to relate θ with ε_a.

The bulk electrical conductivity, σ, is calculated with the long-time TDR waveform analysis, according to

$$\sigma = \frac{K_p}{Z_r}\left(\frac{1-\rho_{\infty,scale}}{1+\rho_{\infty,scale}}\right) \quad (2)$$

where Z_r is the output impedance (50 Ω), K_p (m^{-1}) is the probe-geometry cell constant and $\rho_{\infty,scale}$ is the scaled steady-state reflection coefficient, calculated according to (Lin et al., 2008).

$$\rho_{\infty,scale} = 2\frac{(\rho_{air}-\rho_{SC})(\rho-\rho_{air})}{(1+\rho_{SC})(\rho-\rho_{air})+(\rho_{air}-\rho_{SC})(1+\rho_{air})} + 1 \quad (3)$$

where ρ, ρ_{air} and ρ_{SC} are the long-time reflection coefficients measured in the studied medium, in air and in a short-circuited probe, respectively. An accurate approximation for a three-rod probe cell constant K_p can be calculated from Green and Cashman (1986) and Ball (2002):

$$K_p \approx \frac{1}{4\pi L_{eff}} ln\left(\frac{1}{2b^3}\right) \quad (4)$$

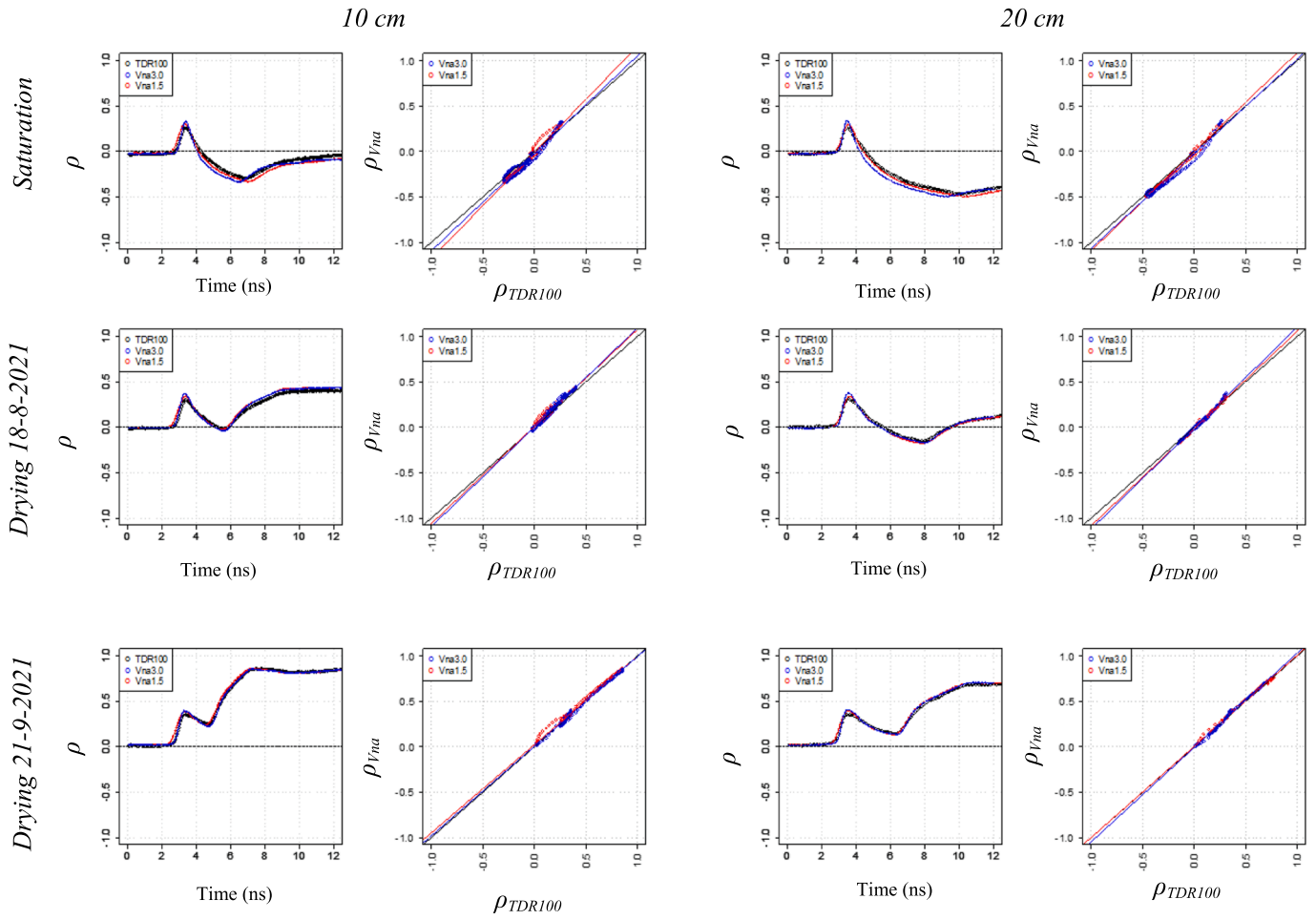

Fig. 2. Comparison of TDR waveforms recorded with TDR100 and VNA1.5 and VNA3.0 devices using 10 cm and 20 cm length TDR probes inserted in saturated soil column and the same column after one and two month of drying.

where

$$b = \frac{r}{s} \tag{5}$$

$$L_{eff} = L + \Delta L \tag{6}$$

and

$$\Delta L \approx \frac{2s}{\sqrt{3.954^2 + \left(2.564 cosh^{-1}\left(\frac{1}{2d}\right)\right)^2 - 3.954}} \tag{7}$$

where r and s denote the rod probe radius and the separation between the central and external rods of the three-rod TDR probe.

3. Material and methods

3.1. Hardware and data acquisition of NanoVNA devices

Several models of low-cost, handheld VNAs are available under the root name NanoVNA. The original version (Takahashi, 2017), designed to operate in the frequency range of 50 kHz to 300 kHz, was latter improved to provide measurements up to 1.5 GHz. Recently, an independent project released VNA models under the name NanoVNA V2 or S-A-A-2 reaching up to 4 GHz. This study evaluates two different small-volume and low-cost NanoVNAs (names of the NanoVNA versions), whose operating frequency ranges from 50 kHz to 1.5 GHz (NanoVNA-H rev4; Hu, 2019) and from 50 kHz to 3 GHz (S-A-A V2; Owotech, 2019), respectively. Both devices include a 2.8-inch touch screen and a 500 mAh battery, which can be used offline for 2 h. For a longer measurement, the analyzer can also be connected to an external power supply. In both cases, data was recorded using the open-source program NanoVNASaver (Broberg, 2019) and the transformation to the time domain was computed with Fast Fourier Transform (FFT) and Inverse Fast Fourier Transform (IFFT) efficient algorithms using the open source Python Numpy library (2021 NumPy; https://numpy.org/). The NanoVNA firmware includes a TDR mode of operation, but its applicability is rather limited as it is focused to test transmission lines of known, uniform electromagnetic wave propagation velocity ending in discrete loads -usually ham radio antennas – and is not flexible enough to be useful for soil characterization.

Before each experiment, both VNA1.5 and 3.0 devices were calibrated following the Open-Short-Load standard calibration procedure (Sayed and Martens, 2013) with the assistance of the NanoVNA firmware.

3.2. Laboratory experiments

A first laboratory experiment was performed to test the accuracy of the VNA devices. To this end, the TDR waveforms and ε_a obtained with the two NanoVNAs were compared to those obtained with a TDR100 (Campbell Scientific Inc., Logan, UT, USA) cable tester. All TDR devices were connected to two three-rod probes (4 mm rod diameter and 48 mm space between the central axis of the outer rods) of 10 and 20 cm effective length, respectively. The first 5 cm of the rods, with a total length of 15 and 25 cm, respectively, were inserted into a PVC probe

Table 1
Regression lines, determination coefficient, R^2 and root means square error, RMSE, values for the comparison between the TDR waveforms recorded with the TDR100 cable tester and the 1.5 and 3.0 GHz Nano-VNA devices connected to a 10 and 20 cm length TDR probes immersed in air and water and inserted in a saturated soil column during a drying process.

		VNA1.5 10 cm			-	VNA1.5 20 cm			-	VNA 3.0 10 cm			-	VNA 3.0 20 cm		
		Regression line	R^2	RMSE		Regression line	R^2	RMSE		Regression line	R^2	RMSE		Regression line	R^2	RMSE
	Air	y = 1.00x – 0.012	0.99	0.027		y = 0.98x + 0.024	0.99	0.044		y = 0.97x + 0.037	0.98	0.056		y = 1.00x – 0.030	0.98	0.060
	Water	y = 0.97x – 0.017	1.00	0.024		y = 0.99x + 0.001	0.99	0.035		y = 0.96x – 0.015	0.99	0.032		y = 0.97x – 0.022	0.97	0.036
	Dry soil	y = 1.00x – 0.018	0.99	0.023		y = 0.98x + 0.010	0.99	0.040		y = 1.01x + 0.031	0.97	0.049		y = 0.96x – 0.017	0.98	0.015
	Saturation soil	y = 0.82x – 0.007	0.97	0.043		y = 0.92x + 0.003	1.00	0.035		y = 0.87x + 0.012	0.93	0.046		y = 0.94x + 0.018	0.98	0.049
Drying process	21/07/2021	y = 0.90x – 0.012	0.98	0.023		y = 0.98x + 0.015	0.99	0.022		y = 0.88x – 0.010	0.98	0.023		y = 0.97x + 0.020	0.98	0.032
	28/07/2021	y = 0.91x – 0.010	0.98	0.022		y = 0.94x + 0.005	1.00	0.022		y = 0.90x – 0.003	0.99	0.017		y = 0.93x + 0.009	0.98	0.037
	09/09/2021	y = 0.89x – 0.006	0.98	0.027		y = 0.95x – 0.011	0.99	0.016		y = 0.89x + 0.001	0.99	0.019		y = 0.98x – 0.006	0.98	0.022
	11/12/2021	y = 0.90x – 0.008	0.98	0.031		y = 0.92x – 0.004	1.00	0.012		y = 0.89x – 0.001	0.99	0.026		y = 0.90x – 0.006	0.95	0.030
	18/08/2021	y = 0.93x – 0.007	0.99	0.033		y = 0.93x + 0.014	1.00	0.014		y = 0.91x + 0.002	0.99	0.030		y = 0.93x – 0.012	0.96	0.020
	20/08/2021	y = 0.93x – 0.004	0.99	0.036		y = 0.92x – 0.001	1.00	0.017		y = 0.92x + 0.007	0.99	0.028		y = 0.87x + 0.001	0.96	0.033
	23/08/2021	y = 0.92x – 0.062	1.00	0.043		y = 0.92x + 0.001	1.00	0.021		y = 0.92x + 0.005	1.00	0.029		y = 0.85x + 0.002	0.95	0.037
	25/08/2021	y = 0.93x – 0.015	1.00	0.046		y = 0.94x – 0.004	1.00	0.021		y = 0.93x – 0.002	1.00	0.034		y = 0.89x – 0.001	0.99	0.026
	30/08/2021	y = 0.95x – 0.012	0.99	0.042		y = 0.93x + 0.002	1.00	0.023		y = 0.94x – 0.004	1.00	0.033		y = 0.90x + 0.005	1.00	0.025
	02/09/2021	y = 0.95x – 0.015	0.99	0.047		y = 0.93x – 0.002	1.00	0.030		y = 0.95x – 0.004	1.00	0.032		y = 0.90x + 0.002	1.00	0.030
	06/09/2021	y = 0.96x – 0.011	0.99	0.040		y = 0.95x + 0.003	1.00	0.022		y = 0.96x + 0.001	1.00	0.025		y = 0.96x + 0.005	0.99	0.018
	08/09/2021	y = 0.97x – 0.014	0.99	0.037		y = 0.95x + 0.001	1.00	0.022		y = 0.97x – 0.002	1.00	0.023		y = 0.93x + 0.010	1.00	0.018
	13/09/2021	y = 0.98x – 0.020	1.00	0.038		y = 0.96x – 0.006	1.00	0.026		y = 0.99x – 0.002	1.00	0.016		y = 0.94x + 0.007	1.00	0.022
	15/09/2021	y = 0.99x – 0.011	0.99	0.025		y = 0.97x – 0.003	1.00	0.023		y = 0.98x + 0.007	1.00	0.016		y = 0.94x + 0.006	1.00	0.024
	21/09/2021	y = 1.00x – 0.023	1.00	0.028		y = 0.99x- 0.004	1.00	0.014		y = 1.00x – 0.004	1.00	0.014		y = 0.96x + 0.007	1.00	0.017

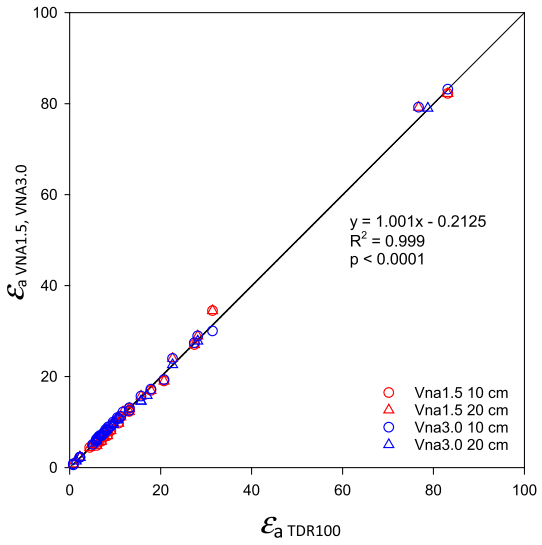

Fig. 3. Relationship between the apparent permittivity estimated with TDR100, $\varepsilon_{a\ TDR100}$, and the VNA1.5 and VNA3.0 devices, $\varepsilon_{a\ VNA1.5,\ VNA3.0}$, connected to a 10 and 20 cm length TDR probes immersed in air and distilled water and the same probes inserted in a soil column with different water content gradient.

Table 2
Regression lines and determination coefficient, R^2, for the relationship between the apparent dielectric constant determined with TDR100 and the corresponding values estimated with the Nano-VNA1.5 and Nano-VNA3.0 devices connected to the 10 cm 20 cm length TDR probes immersed in air, distilled water and inserted in a soil column during a drying process.

		Regression line	R^2
VNA1.5	10 cm	y = 0.99x + 0.012	0.997
	20 cm	y = 1.00x + 0.004	0.998
VNA3.0	10 cm	y = 0.98x + 0.002	0.995
	20 cm	y = 0.99x + 0.002	0.998

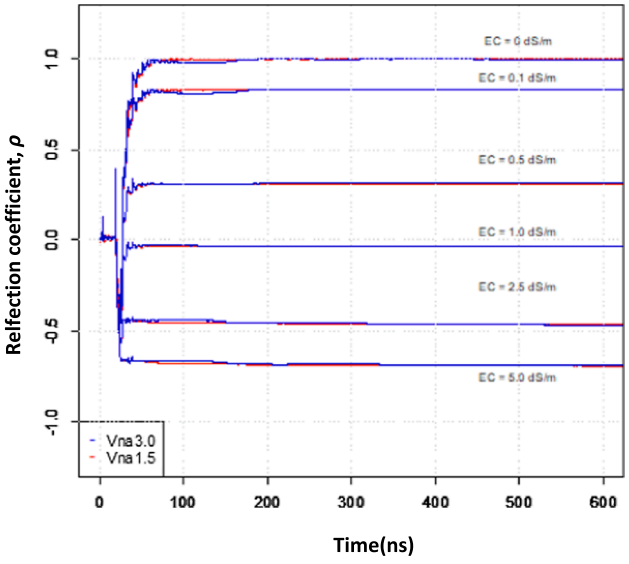

Fig. 4. Long-time TDR waveforms recorded with VNA1.5 and VNA3.0 devices connected to a 10 cm length three-rod TDR probe immersed distilled water and five different NaCl-water solutions.

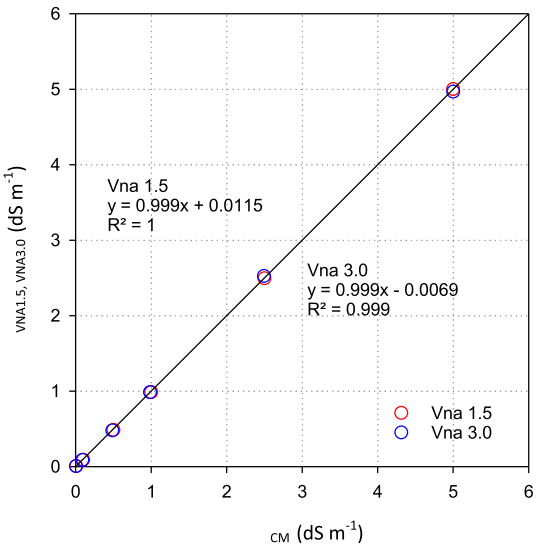

Fig. 5. Relationship between the apparent bulk electrical conductivity measured with the conductivity meter, σ_{CM}, at different NaCl-water solutions and the corresponding values estimated with the VNA1.5, $\sigma_{VNA1.5}$, and VNA3.0, $\sigma_{VNA3.0}$, devices, connected to a 10 cm length three-rod TDR probe.

head (4 cm high, 9 cm wide, and 2 cm thick). The remaining 1-cm of rod protruding above the PVC block was connected to a coaxial cable 0.5 cm in diameter and 150 cm long. The inner cable and outer sheath of the coaxial cable were soldered to the central rod and external rods, respectively. The end of the coaxial cable was finally soldered to a BNC connector. Although the BNC was connected directly to the TDR100, a BNC-SMA adapter was required to connect the coaxial cable to the VNAs. The two probes were immersed in distilled water and air, and inserted in a soil column with different water contents. In the soil column experiment, the two probes were vertically inserted in a 25 cm high and diameter cylinder filled with 2 mm sieved and air-dried loam. An initial measurement was performed in the dry soil column. Next, the column, which has a drain at the bottom, was wetted until the water started to drain by the base. Under these conditions, which corresponded to soil saturation, a second measurement was performed. From this moment, additional TDR waveforms were recorded during several weeks as the soil dried. A total of 14 measurements, from saturation to dry soil, were registered.

The Wifi-TDR (Villoro et al., 2021) system was employed to record TDR waveforms with the TDR100 cable tester. While TDR100 can move and zoom the analysis window to fix the TDR signal between the first peak and the second reflection point (i.e. Fig. 1), no zooming was possible with the NanoVNAs. No calibration of the cable length was needed. Each of the two probes were soldered to a different coaxial cable which was connected either to the TDR100 or the NanoVNA devices. This design resulted in the probes remaining fixed during the experiment. In all cases, the section of the TDR waveform used to estimate θ was located between the first peak and the second reflection point (Fig. 1). The first peak of the TDR waveform was calculated as the intersection of the regression lines from both sides of the maximum value. The second reflection point was located from the intersection between the horizontal line corresponding to the minimum TDR signal value and the line from the maximum slope point found after this minimum value. Given that TDR100 waveforms presents higher density of points than the NanoVNA devices, direct comparison between them required to interpolate the NanoVNA signals to the TDR100 temporal resolution. To this end, a cubic interpolation method was applied to the VNA TDR waveforms. Subsequently, the interpolated VNA TDR waveforms were used to estimate ε_a using the tangent method.

A second laboratory experiment was performed to evaluate the accuracy of the VNA devices to estimate σ. This consisted of comparing σ measured with both NanoVNA connected to the 10 cm length probe immersed in increasing NaCl-water solutions with the reference values determined using an electrical conductivity cell, CM (Conductivity meter 522, Crison Instruments, Barcelona). To this end, K_p for each NanoVNA was optimized from the best fit between σ measured with the conductivity meter and the corresponding values calculated with Eq.(2). The probe was immersed in a cylindrical clear plastic container (30 cm i. d. and 30 cm in height) filled with deionized water (0.007 dS m^{-1}) and five increasing NaCl-water solutions with electrical conductivities of 0.1, 0.5, 1.0, 2.5, and 5 dS m^{-1} at 25 °C. For these measurements, the section corresponding to the long-time TDR waveform was selected. Finally, optimized K_p were compared with the corresponding theoretical value calculated according to Eq.(4). While TDR100 allowed decreasing the window zoom to select long-time reflection values, in the case of NanoVNA, the long-time signal was obtained by adding successive TDR waveform records.

3.3. Field experiments

The VNA devices were tested in a field trial in order to determine θ in five 0.5 m^2 plots with increasing water contents. The perimeter of the plots was limited by a small earthen wall 5 cm-high. Within each plot, two two-rod 25-cm long probes (0.5 cm rod diameter and 4 cm space between the central axis of the rods) were vertically inserted to a depth of 22 cm, remaining 3 cm of the probe end in contact with air. The top end of the probes were connected to the TDR100 and NanoVNA via an interchangeable clamp interface, which in turn was connected to the end of a coaxial cable 0.5 cm in diameter and 120 cm long. This means that the same coaxial cable was employed in all measures. The soil, which was initially dry (≅0.03 cm^3 cm^{-3}), was previously tilled with a

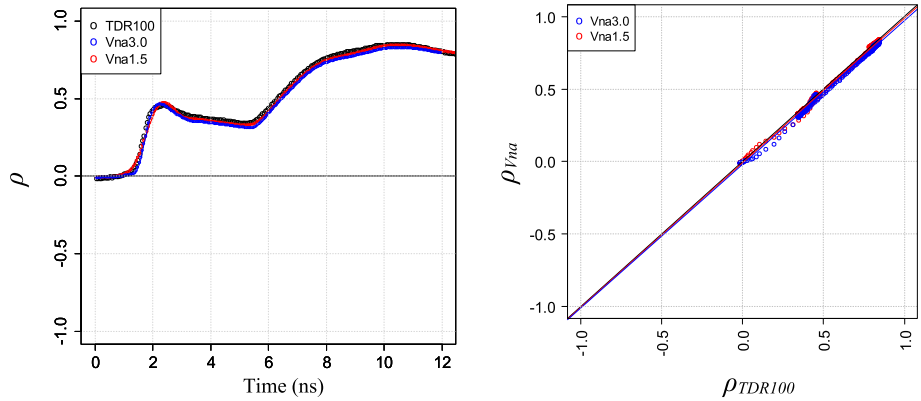

Fig. 6. Comparison of TDR waveforms recorded from field experimental plot watered with 2 l of water using TDR100 and VNA1.5 and 3.0 devices.

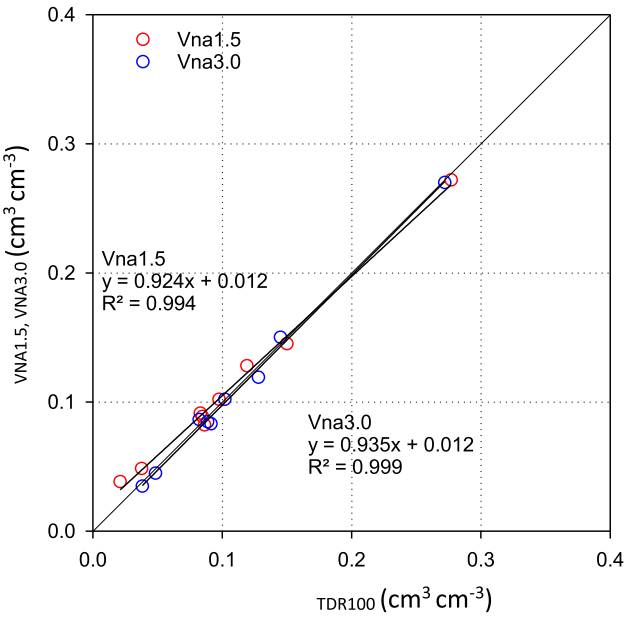

Fig. 7. Relationship between volumetric water content, θ, measured in the field experiment with TDR100, θ_{TDR100}, and the VNA1.5 and VNA3.0 devices, $\theta_{VNA1.5,\ VNA3.0}$.

rototiller. While the first plot was left as dry soil, the remaining plots were watered by applying 1, 2, 5 and 10 l of water within the perimeter of each plot, respectively, 24 h before the measurements. While the TDR-WiFi (Villoro et al., 2021) device was employed to acquire the TDR100 waveforms, NanoVNA FDR data were recorded using a laptop. The first series of measurements performed with the TDR100 were followed by VNA1.5 and VNA3.0 measurements.

4. Results and discussion

TDR waveforms registered with both NanoVNA devices and the TDR100 using a 10 cm length probe immersed in distilled water shows that the number of points per waveform follows the gradient TDR100 ≫ VNA3.0 > VNA1.5 (Fig. 1). For instance, while TDR100 registered 254 points within the [0, 13] ns interval, the number of points decreased to 81 and 41 for VNA3.0 and VNA1.5, respectively. These differences are consequence of the lower temporal resolution of the NanoVNA devices, as explained in Section 2, showing that higher frequency devices allow a better temporal resolution of the TDR waveform. Given that both TDR100 and NanoVNA waveforms presented different temporal resolution, from now on, comparisons will be made after interpolating the VNA waveforms to the TDR100 temporal resolution.

Overall, a robust fit was observed between TDR waveforms recorded with TDR100 in the soil column experiment and the corresponding interpolated signals from the two NanoVNA devices (Fig. 2). The high R^2 and low RMSE values, together with the close to one regression lines slope (Table 1) indicates the VNA devices offer accurate reconstruction of TDR waveforms. Similarly, the robust relationship between the ε_a measured with TDR100 and the NanoVNA devices (Fig. 3), demonstrates these alternative low-cost cable testers can measure ε_a with similar accuracy and precision as the TDR. Although VNA3.0 presents double frequency than VNA1.5, no significant differences in the ε_a estimation were observed (Table 2). Given that θ is directly related to ε_a, these results can be extrapolated, affirming that both VNA3.0 and VNA1.5 also allow accurate determinations of the soil water content within the tested experimental conditions. These results, which significantly improve those obtained by Qiwei et al. (2019), could be attributed to the 3-rod probe used in our experiment, which probably made possible a better analysis of the TDR signal.

Overall, no significant differences were observed between the long-time TDR waveforms used to estimate σ and recorded with the VNA1.5 and VNA3.0 connected to the 10 cm length probe immersed in different NaCl-solutions (Fig. 4). Given that σ estimation depends only on the stationary section of the TDR waveform, unlike the TDR signal used for water content determination, the higher frequency with VNA3.0 did not result in better estimates of σ. In this case, both devices resulted in an accurate determination of σ (Fig. 5). The constant cell values experimentally optimized from σ_{CM} vs σ_{VNA} relationship (45.5 m^{-1} for both VNA1.5 and VNA3.0) were close to the theoretical value of 46.77 m^{-1} calculated according to Eq. (4). These small differences between theoretical and optimized K_p values, which should be attributed to the presence of sharp edges in the probe tips and to small differences in gain between input stages, confirm the robustness of the NanoVNA devices for measuring σ.

The satisfactory results obtained with the NanoVNA devices in laboratory were supported by the field experiments, where TDR waveforms recorded with NanoVNA instruments connected to two-rod 22 cm length probes matched well with the corresponding signals registered with the TDR100 (Fig. 6). Also, a robust relationship was observed between the θ estimated with the TDR100 and those measured with the two NanoVNA devices (Fig. 7). Although no significant differences were found between VNA1.5 and VNA3.0 devices, the slightly better results obtained with VNA3.0 can be attributed to the higher frequencies offered by this device. Compared with the laboratory experiments, the differences found in the field trial (Fig. 3 vs Fig. 7) can be attributed to the coaxial cable connection employed in both experiments. Unlike the laboratory experiment, where the probes remained fixed, the interchangeable clamp interface used in the field could cause small displacements of the TDR rods and hence affecting the water content measurements. However, despite these small differences, field results were, overall, satisfactory and indicate that the low-cost NanoVNA devices are an accurate alternative for measuring θ.

5. Conclusions

This study evaluates two different low-cost FDR-TDR devices NanoVNA, from 50 kHz to 1.5 GHz (VNA1.5) and from 50 kHz to 3.0 GHz (VNA3.0), for measuring the soil volumetric water content and the bulk electrical conductivity. The ε_a estimated with both NanoVNA devices connected to a 10 and 20 cm length three-rod probes immersed in water, air and inserted in soil column with different water contents was satisfactorily compared with the corresponding values measured using a TDR100 (Campbel Sci.) cable tester. In addition, the σ measured with a conductivity meter in different NaCl-water solutions also agreed with the corresponding values measured using a 10 cm length TDR probe connected to the VNA devices. These results are supported by a field trial, demonstrating that the evaluated devices result in accurate measurements of both θ and σ. These results indicate that these low-cost instruments (€ 50–100 $unit^{-1}$), which can indistinctly run with 2- or 3-rod probes, can be a robust alternative for water content measurement, and can expand the TDR applications. On the other hand, the small volume of these devices, which can also be connected to a smartphone, result in a portable and easy handling instrument. Finally, the easy operation of the NanoVNA instruments allows the users to calibrate them in a simple and fast way. The characteristics of the evaluated devices, along with the versatility of the TDR technique, which can connect a same instrument very different types probes, makes these devices have great potential for soil research. However, one limitation of these new devices is that no zooming of TDR waveforms was possible. On the other hand, although both NanoVNA presented good results when connected to a 10 and 20 cm-length TDR probe, further efforts should be done to test its accuracy on shorter probes. In addition, it would be interesting to study the behavior of these devices outdoors considering, for instance, the effect of extreme temperatures or relative humidity on soil moisture measurements.

Declaration of Competing Interest

The authors declare that they have no known competing financial interests or personal relationships that could have appeared to influence the work reported in this paper.

Data availability

Data will be made available on request.

Acknowledgements

This work is based on the idea originally proposed by Dr. José Vicente, who was unable to participate in the list of authors. This research was partially supported by the MITECO project ASBIO (PGC2018-094332-B-100).

References

Ball, J.A.R., 2002. Characteristic impedance of unbalanced TDR probes. IEEE Trans. Instr. Meas. 51 (3), 532–536.

Broberg, R., 2019. NanoVNASaver - A multiplatform tool to save Touchstone files from the NanoVNA, sweep frequency spans, and generally display and analyze the resulting data. GitHub repository. https://github.com/NanoVNA-Saver/nanovna-saver.

Cooley, J.W., Tukey, J.W., 1965. An algorithm for the machine calculation of complex Fourier series. Math. Comput. 19 (90), 297–301.

Evett, S.R., 2000. The TACQ computer program for automatic time domain reflectometry measurements: Waveform interpretation methods. Trans. ASAE 43, 1947–1956.

Friel, R., Or, D., 1999. Frequency analysis of time-domain reflectometry (TDR) with application to dielectric spectroscopy of soil constituents. Geophysics 64 (3), 707–718.

González-Teruel, J.D., Jones, S.B., Robinson, D.A., Giménez-Gallego, J., Zornoza, R., Torres-Sánchez, R., 2022. Measurement of the broadband complex permittivity of soils in the frequency domain with a low-cost Vector Network Analyzer and an Open-Ended coaxial probe. Comput. Electron. Agric. 195, 106847.

Greco, R., 2006. Soil water content inverse profiling from single TDR waveforms. J. Hydrol. 317, 325–339.

Green, H.E., Cashman, J.D., 1986. End effect in open-circuited two wire transmission lines. IEEE Trans. Microwave Theory Techniques 34, 180–186.

He, H., Aogu, K., Li, M., Xu, J., Sheng, W., Jones, S.J., González-Teruel, J.D., Robinson, D.A., Horton, R., Bristow, K., Dyck, M., Filipovic, W., Noborio, K., Wu, Q., Jin, H., Feng, H., Si, B., Lv, J., 2021. A review of time domain reflectometry (TDR) applications in porous media. Adv. Agr. 168 https://doi.org/10.1016/bs.agron.2021.02.003.

Heimovaara, T.J., 1993. Design of triple-wire time domain reflectometry probes in practice and theory. Soil Sci. Soc. Am. J. 57 (6), 1410–1417.

Heimovaara, T.J., 1994. Frequency domain analysis of time domain reflectometry waveforms. 1. Measurement of the complex dielectric permittivity of solids. Water Resour. Res. 30 (2), 189–199.

Hu, G., 2019. NanoVNA-H - Handheld Vector Network Analyzer. GitHub Repository. https://github.com/hugen79/NanoVNA-H.

Huisman, J.A., Weerts, A.H., Heimovaara, T.J., Bouten, W., 2002. Comparison of travel time analysis and inverse modeling for soil water content determination with time domain reflectometry. Water Resour. Res. 38 (6), 13-1.

Huisman, J.A., Bouten, W., Vrugt, J.A., Ferré, P.A., 2004. Accuracy of frequency domain analysis scenarios for the determination of complex dielectric permittivity. Water Resour. Res. https://doi.org/10.1029/2002WR001601.

Jones, S.B., Wraith, J.M., Or, D., 2002. Time Domain Reflectometry (TDR) Measurement Principles and Applications. Hydrol. Process. 16, 141–153.

Lin, C.-P., Chung, C.-C., Huisman, J.A., Tang, S.-H., 2008. Clarification and calibration of reflection coefficient for electrical conductivity measurement by time domain reflectometry. Soil Sci. Soc. Am. J. 72 (4), 1033–1040.

Miyamoto, R., Kobayashi, R., Annaka, T., Chikushi, J., 2001. Applicability of multiple length TDR probes to measure water distributions in an Andisol under different tillage systems in Japan. Soil Till. Res. 60, 91–99.

Moret-Fernández, D., Vicente, J., Lera, F., Latorre, B., López, M.V., Blanco, N., González-Cebollada, C., Arrúe, J.L., Gracia, R., Salvador, M.J., Bielsa, A., 2010. TDR-Lab Version 1.0 Users Guide (http://digital.csic.es/handle/10261/35790).

Moret-Fernández, D., Vicente, J., Aragüés, R., Peña, C., López, M.V., 2012. A new TDR probe for measurements of soil solution electrical conductivity. J. Hydrol. 448–449, 73–79.

Oppenheim, A.V., Willsky, A.S., Nawab, S.H., 1997. Signals & Systems, 2nd ed. Prentice-Hall, Upper Saddle River, N.J., USA.

Or, D., Wraith, J.M., 1999. A new soil metric potential sensor based on time domain reflectometry. Water Resour. Res. 35 (11), 3399–3407.

OwOTech, 2019. NanoVNA V2 (S-A-A-2)- 4GHz vector network analyzer (VNA) capable of measuring antennas, filters, duplexers, and amplifiers. GitHub repository. https://github.com/nanovna-v2/NanoVNA2.

Qiwei, Z., Zainuddin, M.F., Ahmad, A.F., Obays, S.J., Abbas, Z., 2019. Development of an Affordable Soil Moisture Sensor System with Mini-VNA Tiny and Smartphone. J. Sci. Technol. 27, 1121–1129.

Sayed, M., Martens, J., 2013. Vector network analyzers. In: Teppati, V., Ferrero, A., Sayed, M. (Eds.), Modern RF and Microwave Measurement Techniques (The Cambridge RF and Microwave Engineering Series). Cambridge University Press, Cambridge, pp. 98–129.

Selker, J.S., Graff, L., Steenhuis, T., 1993. Noninvasive time domain reflectometry moisture measurement probe. Sci. Soc. Am. J. 57, 934–936.

Takahashi, T., 2017. NanoVNA - Handheld Vector Network Analyzer. GitHub Repository. https://github.com/ttrftech/NanoVNA.

Topp, G.C., Davis, J.L., Annan, A.P., 1980. Electromagnetic determination of soil water content: Measurements in coaxial transmission lines. Water Resour. Res. 16 (3), 574–582.

Topp, G.C., Davis, J.L., Annan, A.P., 1982. Electromagnetic determination of soil water content using TDR: II. evaluation of installation and configuration of parallel transmission lines. Soil Sci. Soc. Am. J. 46 (4), 678–684.

Villoro, A., Latorre, B., Tormo, J., Jiménez, J.J., López, M.V., Nicolau, J.M., Vicente, J., Gracia, R., Moret-Fernández, D., 2021. A TDR wireless device for volumetric water content sensing. Comput. Electron. Agric., 10.1016/j.compag.2020.105939.